Atmospheric Science Letters

RMetS Royal Meteorological Society

RESEARCH ARTICLE OPEN ACCESS

Variability of Tropical Cyclogenesis in the Bay of Bengal Across the Phase Space of the Madden–Julian Oscillation

Bradford S. Barrett[1] | Nadim Mahmud[2] | Md Masud-Ul-Alam[2,3] | Pallav Ray[4] | Sahadat Habib[5] | Md Foysal[5] | Most Israt Jahan Mili[6] | Md Hanif Biswas[7]

[1]Independent Scholar, Raleigh, North Carolina, USA | [2]Department of Oceanography and Hydrography, Bangladesh Maritime University, Dhaka, Bangladesh | [3]Skidaway Institute of Oceanography, University of Georgia, Savannah, Georgia, USA | [4]Meteorology, Ocean Engineering, and Marine Sciences, Florida Institute of Technology, Melbourne, Florida, USA | [5]Department of Oceanography, University of Dhaka, Dhaka, Bangladesh | [6]School for Marine Science and Technology, University of Massachusetts, Dartmouth, Massachusetts, USA | [7]Bangladesh Oceanographic Research Institute, Cox's Bazar, Bangladesh

Correspondence: Nadim Mahmud (mahmudnadim8@gmail.com)

Received: 10 December 2025 | **Revised:** 23 May 2026 | **Accepted:** 5 June 2026

Keywords: bay of Bengal (BoB | intraseasonal variability | Madden–Julian oscillation (MJO) | RMM index | tropical cyclone (TC)

ABSTRACT

In this study, probabilities of tropical cyclogenesis in the Bay of Bengal (BoB) were analyzed across the full two-dimensional phase space of the real-time multivariate Madden–Julian oscillation (MJO) (RMM) index for pre- and post-monsoon periods from 1990 to 2025. Results show that cyclogenesis anomalies span the phase space and depend largely on the sign of the first principal component of the index, RMM1. Moreover, on days when the intraseasonal index is in phases previously found favorable for cyclogenesis, the anomalies are statistically significant for only a limited range of amplitudes in those phases. Skill scores were calculated for vertical velocity (VV), relative humidity (RH), sea level pressure (SLP), vertical wind shear (VWS), and sea surface temperature (SST) to quantify how well each parameter identifies cyclogenesis in the intraseasonal phase space. Among these variables, 700-hPa VV was most skillful at identifying both pre- and post-monsoon cyclogenesis anomalies, outperforming RH, SLP, VWS, and SST, although all had high false alarm ratios. The 700-hPa VV was also more skillful than the 500-hPa VV, suggesting that it should be included in intraseasonal genesis indices. In the post-monsoon period, SST showed little to no skill at identifying intraseasonal cyclogenesis anomalies, in agreement with recent work suggesting it be considered alongside other modes of variability. The results of this study fill a critical gap in our understanding of the MJO–tropical cyclone relationship in the BoB by establishing basin-specific probabilities of cyclogenesis across multiple MJO states and identifying drivers of the variability.

1 | Introduction

Tropical cyclones (TCs) are one of the deadliest and most destructive weather phenomena on Earth. Tropical cyclogenesis often occurs when the large-scale environment favors TC development, with high mid-tropospheric relative humidity (RH) (Pal and Chatterjee 2021), cyclonic lower-tropospheric relative vorticity (Duan et al. 2021), low vertical wind shear (VWS) (Hoarau et al. 2012; Suneeta et al. 2026), and warm sea surface temperatures (SSTs) (Balaguru et al. 2014; Maneesha et al. 2025). In the Bay of Bengal (BoB), on average, three to four incipient disturbances (Li et al. 2019; Hossain et al. 2024) develop into TCs each year (Balaguru et al. 2014; Alam and Dominey-Howes 2015; Bhardwaj and Singh 2020). While many recent studies have found that intraseasonal variability projects onto cyclogenesis in the BoB via controls on the large-scale environment (Sattar and Cheung 2019; Roman-Stork and Subrahmanyam 2020; Singh et al. 2021; Ipsita et al. 2023; Gorja

et al. 2025; Paul et al. 2025), basin-specific details remain unclear. Such work is valuable because it unlocks intraseasonal predictions of TC impacts (Robertson et al. 2020), which is especially crucial for the BoB, where there is an urgent need for accurate forecasts to mitigate the often very high societal costs from TCs (Kabir et al. 2022; Matin et al. 2024; Wahiduzzaman and Yeasmin 2024; Zhou et al. 2025) and their projected increase in the future (Mittal et al. 2019).

One of the leading drivers of atmospheric and oceanic intraseasonal variability in the BoB is the Madden–Julian oscillation (MJO) (Madden and Julian 1971, 1972). Past studies of the climatological relationship of the MJO to tropical cyclogenesis have reported sharp regional differences in the large-scale environment that depend strongly upon the position and intensity of the MJO convection and circulation (Zhao and Li 2019). Thus, it is acutely important to establish environments in the BoB across a range of MJO states (Rahul et al. 2022). The real-time multivariate MJO (RMM) index (Wheeler and Hendon 2004) is one tool used widely to characterize the state of the MJO. The RMM index is generated by projecting anomalies of outgoing longwave radiation and zonal 850- and 200-hPa winds between 15N and 15S onto the two leading principal components (RMM1 and RMM2) of an empirical orthogonal analysis (Gottschalck et al. 2010). Together, RMM1 and RMM2 form a two-dimensional phase space that captures the location and intensity of the MJO convection and the quasi-cyclic eastward progression of its circulation (Lafleur et al. 2015; Jiang et al. 2020).

In MJO–TC studies that use the RMM index, an amplitude threshold is often applied to identify active MJO events, after which composites of key variables are constructed for the active phases. Using this approach, Bhardwaj et al. (2019) found that cyclogenesis in the BoB is more likely on days when the RMM index is in Phases 2–4 and less likely when the index is in Phases 7–1. They found below-normal sea level pressure (SLP), above-normal RH, and below-normal VWS during Phases 2–4. Krishnamohan et al. (2012), Girishkumar et al. (2015), Rahul et al. (2022), and Chen et al. (2024) used similar methods with corroborating results. Nevertheless, the variability of cyclogenesis across the full phase space (and not just in one of the active phases) is unclear, despite skillful predictions of the MJO out to 4 weeks (Kim et al. 2018, 2026) that have led to routine use of the RMM index to predict tropical cyclogenesis (Schreck III et al. 2023). The purpose of this study is to fill this gap by more completely characterizing the relationship of the MJO to cyclogenesis in the BoB across the full RMM phase space.

2 | Data and Methods

TC latitude, longitude, and sustained 10-m, 1-min average wind speed were retrieved every 6 h (0000, 0600, 1200, and 1800 UTC) from the International Best Track Archive for Climate Stewardship (IBTrACS; Gahtan et al. 2024; Knapp et al. 2010) version 4.01 from 1990 to 2025. We began our analysis in 1990 to correspond approximately with the routine availability of geostationary infrared imagery over the BoB (Kelkar 2019). Cyclogenesis was defined as the first moment a TC reached tropical storm strength with a wind speed of at least 34 kt. The TC record for this study was separated into pre- and post-monsoon periods following Bhardwaj and Singh (2020), and 21 TCs were identified in the BoB during the pre-monsoon period from April 21 to May 31 while 60 TCs were identified in the post-monsoon period from October 1 to December 10 (Figure 1a–c).

A bivariate Gaussian kernel density estimate (KDE) of the probability of cyclogenesis was calculated across the RMM phase space following Cao (2025), and probability anomalies were calculated by subtracting the KDE of the probability of an MJO day from the KDE of the probability of cyclogenesis. Bootstrap sampling with replicates was applied 1000 times to the genesis anomalies to obtain the probability distribution, which was then tested for statistical significance using a Welch's *t*-test.

Five environmental variables known to be associated with cyclogenesis in the BoB were selected for analysis: vertical velocity (VV) at 700 hPa, mid-tropospheric RH (averaged every 50 hPa between 850 and 500 hPa), SLP, deep-layer VWS (the 200-hPa vector wind minus the 850-hPa vector wind), and SST. The environmental data were obtained from the fifth-generation global reanalysis product (ERA5; Hersbach et al. 2020) and the L4 global SST analysis (Embury et al. 2024) from 1990 to 2025. Anomalies were calculated by removing the respective pre- or post-monsoon mean.

The state of the MJO was defined according to the RMM index, where amplitude is given as $(\mathrm{RMM1}^2+\mathrm{RMM2}^2)^{0.5}$. Environmental anomalies were averaged over the BoB (5N–20N, 80E–100E), projected onto RMM phase space using a triangle-based cubic spline interpolation, and tested for statistical significance using a Student's *t*-test. To quantify the relationship between each variable and cyclogenesis, skill scores were calculated, with a "hit" defined as a statistically significant ($p<0.05$) environmental anomaly co-located in RMM phase space with a statistically significant genesis anomaly. A "miss" was defined as a statistically significant genesis anomaly not co-located in phase space with a statistically significant environmental anomaly. A "false alarm" was defined as a statistically significant environmental anomaly not co-located with a statistically significant genesis anomaly. From those definitions, the probability of detection (POD), false alarm rate (FAR), and critical success index (CSI) were calculated (Wilks 2011).

3 | Results

3.1 | Tropical Cyclogenesis

In the pre-monsoon period, the probability of cyclogenesis decreased radially with increasing RMM index amplitude and was highest on days when RMM1 is positive and the amplitude is between 0 and 1.2 (Figure 2a). The probability of cyclogenesis was statistically significantly above normal on days when RMM1 is positive and the index amplitude is greater than 1.2 (Figure 2c) and below normal on days when either the amplitude of the index is less than one or when RMM1 is negative and the index amplitude is greater than one. This pattern shifted some in the post-monsoon period. Cyclogenesis was most likely on days when RMM1 is positive, RMM2 is negative, and the index amplitude is between 0–1.2 (Figure 2b). The probability of post-monsoon cyclogenesis was statistically significantly below

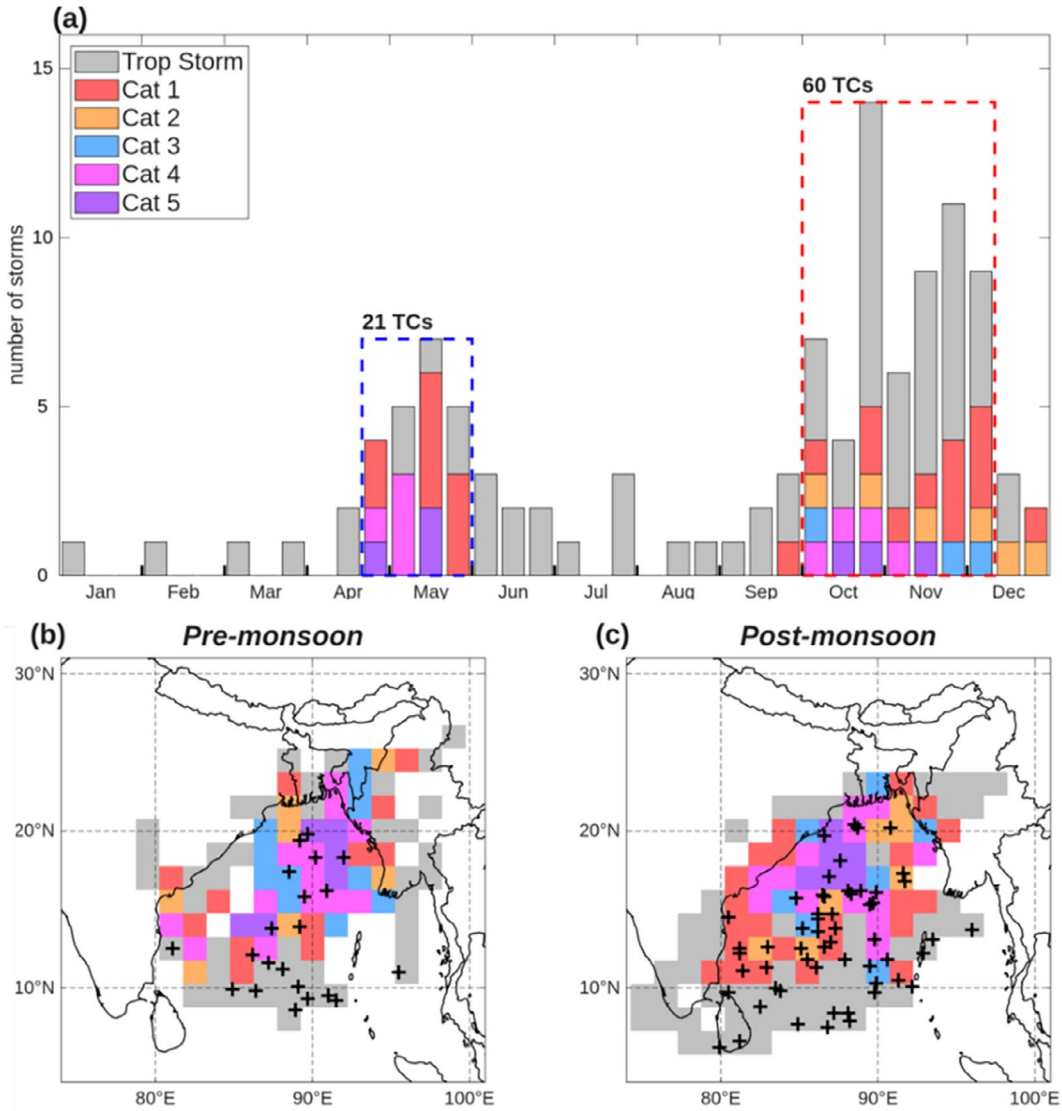

FIGURE 1 | (a) Counts and maximum intensities of TCs in the BoB from 1990 to 2025. The blue dashed box highlights the 21 TCs that formed in the pre-monsoon period, while the red dashed box highlights the 60 TCs that formed in the post-monsoon period. Maximum intensity in each latitude-longitude box is shaded, and cyclogenesis is indicated by + symbols for the (b) pre- and (c) post-monsoon periods. Intensity categories are defined using the Saffir-Simpson wind scale (Taylor et al. 2010).

normal when RMM1 is negative, especially when the index amplitude is between 0.75 and 1.75.

These results refine the work of Tsuboi and Takemi (2014), Girishkumar et al. (2015), Bhardwaj et al. (2019), Singh et al. (2021), Rahul et al. (2022), and Chen et al. (2024), who all found enhanced cyclogenesis in the BoB on days when the RMM index is in Phases 3–4. Here, we show that anomalous probabilities of cyclogenesis span the full RMM phase space, not only Phases 3–4 (Figures 2c–d), and depend most strongly on the sign of RMM1 in both periods. Furthermore, even on days when the index is in Phases 3–4, cyclogenesis anomalies are statistically significant only for a narrow range of amplitudes that varies between pre- and post-monsoon periods. This dependence of cyclogenesis on index intensity is potentially related to the projection of progressively stronger convectively reinforced circulations onto the local environment (e.g., Tromeur and Rossow 2010).

3.2 | Environmental Anomalies Across RMM Phase Space

3.2.1 | Vertical Velocity

During the pre-monsoon period, VV anomalies at 700 hPa were statistically significantly negative (upward) (up to $-0.05\,\mathrm{hPa\,s^{-1}}$) primarily on days when RMM1 is positive and the index amplitude is greater than one (Figure 3a). They were statistically significantly positive (downward) ($0.02–0.04\,\mathrm{hPa\,s^{-1}}$) on days when RMM1 is negative and the index amplitude is greater than one. During the post-monsoon period, VV anomalies were statistically significantly negative (up to $-0.02\,\mathrm{hPa\,s^{-1}}$) on days when RMM1 > RMM2 and the index amplitude is greater than 0.8 (Figure 3b). They were statistically significantly positive ($0.02–0.05\,\mathrm{hPa\,s^{-1}}$) when RMM2 > RMM1 and the index amplitude is greater than 0.7. VV anomalies at 500 hPa are similar to 700 hPa in both periods (Figure 3c–d), although the

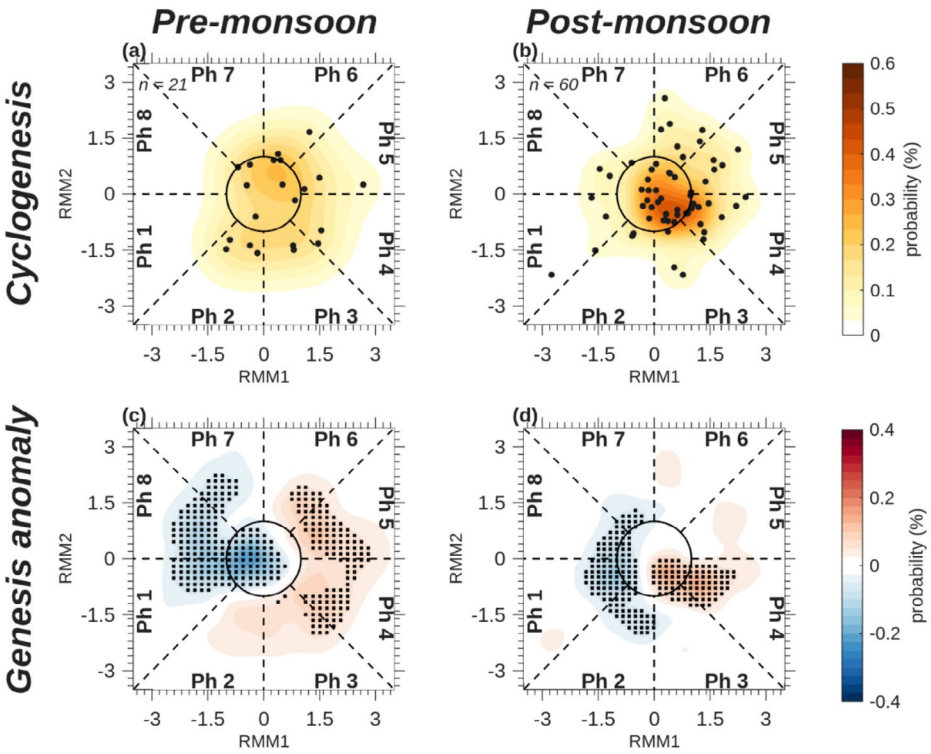

FIGURE 2 | (a, b) Probability of cyclogenesis (in %) across RMM space for the pre- and post-monsoon periods, respectively. Genesis events are indicated by black circles. (c, d) Anomalous probability of cyclogenesis (in %) for the pre- and post-monsoon periods, respectively. Stippling indicates anomalies that are statistically significant at the 95% level.

signal is not as clear, with downward anomalies present even when RMM1 > RMM2. These results extend the work of Bao et al. (2025), who found intraseasonal variability of VV across the global tropics for active MJO events. Here, we show that VV anomalies in the BoB span the full phase space. The intensity of the VV anomalies is proportional to the magnitude of RMM1, in good physical agreement with the loading pattern of deep convection of the first principal component (Wheeler and Hendon 2004).

3.2.2 | Relative Humidity

During the pre-monsoon period, RH anomalies were statistically significantly positive (3%–7% above normal) on days when RMM1 > RMM2 and statistically significantly negative (2%–5% below normal) on days when RMM1 < RMM2 (Figure 4a). Both positive and negative anomalies occurred primarily when the index amplitude is greater than about 1.3. During the post-monsoon period, RH anomalies were statistically significantly positive (up to 5% above normal) in a disjointed region across the phase space, with the strongest positive anomalies on days when the index amplitude is greater than 1.5 and RMM1 > RMM2 (Figure 4b). RH anomalies were statistically significantly negative (up to 10% below normal) on days when RMM1 is positive and the index amplitude is greater than two and RMM2 > RMM1.

These results corroborate the work of both Chen et al. (2024), who found water vapor flux convergence (and above-normal RH) in the lower troposphere on pre-monsoon days when the index was in Phases 3–6 and flux divergence on days the index was in Phases 7–2, and Rahul et al. (2022), who found above-normal RH in the BoB during Phases 2–5. We show that the index amplitude is critically important in those phases, as anomalies are only statistically significant when the amplitude is greater than 1.3 (pre-monsoon) period and 2 (post-monsoon). This dependence on index amplitude was also observed in the 700-hPa VV (Figure 3a–b).

3.2.3 | SLP

During the pre-monsoon period, SLP anomalies were statistically significantly negative (1–3 hPa below normal) on days when RMM1 + RMM2 > 0 and the index amplitude is greater than 1 (Figure 4c). They were statistically significantly positive (2–3 hPa above normal) when RMM1 + RMM2 < 0 and the index amplitude is greater than 2. During the post-monsoon period, SLP anomalies were statistically significantly negative (2–3 hPa below normal) on days when RMM1 is positive and the index amplitude is greater than 1.3, and they were statistically significantly positive (2–3 hPa above normal) when RMM1 is negative and the index amplitude is greater than 1.5 (Figure 4d).

This result both corroborates and extends Bhardwaj et al. (2019), who found below-normal SLP during Phases 3–6 and above-normal SLP during Phases 7–1 in both pre- and post-monsoon periods. As with VV and RH, here we show that significant SLP anomalies extend throughout the RMM phase space. However, when the index is in the phases identified by

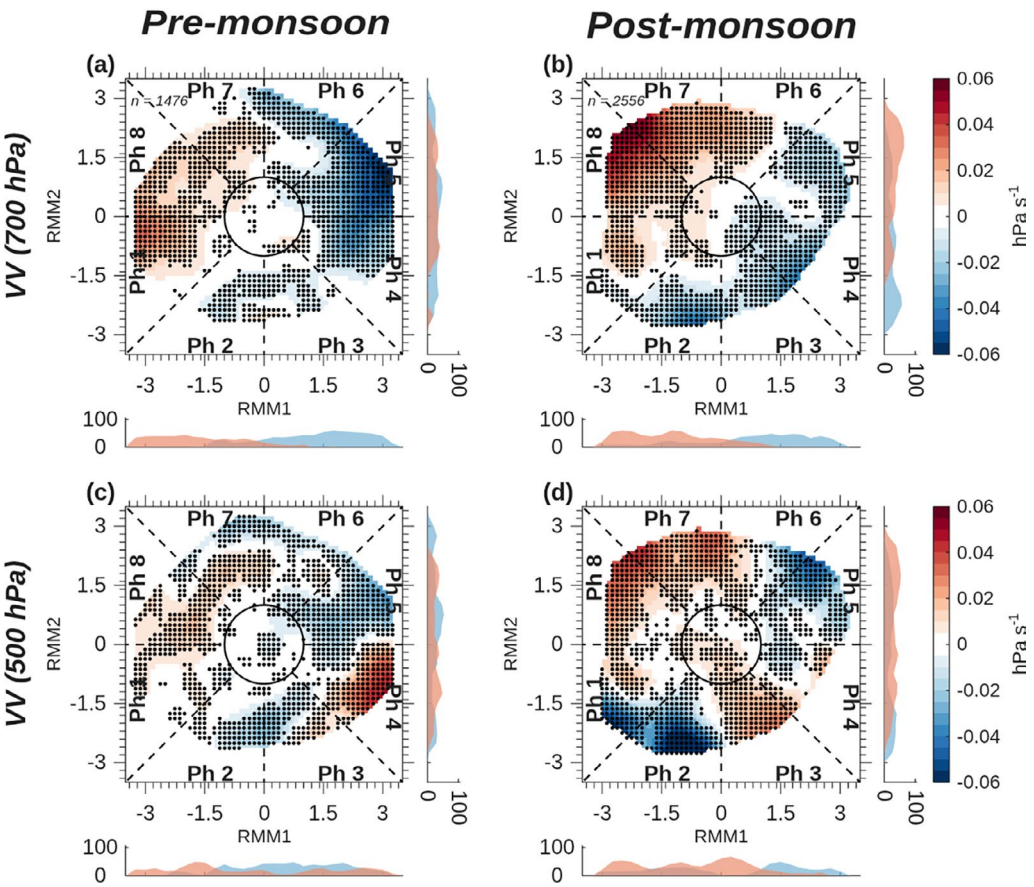

FIGURE 3 | Anomalies of vertical velocity (VV) at (a, b) 700 hPa (in hPa s^{-1}) and (c, d) 500 hPa (in hPa s^{-1}) across RMM phase space for the pre- and post-monsoon periods, respectively, in the BoB. The number of days in each period is given by *n*. Stippling indicates anomalies that are statistically significant at the 95% level. Counts of statistically significant positive (red) and negative (blue) grid points of RMM1 and RMM2 are given in horizontal and vertical histograms, respectively.

Bhardwaj et al. (2019) with anomalous cyclogenesis, we found that SLP anomalies are statistically significant only when the index amplitude is greater than about 1.5. This dependence on index amplitude indicates that the convectively reinforced circulations project onto SLP, VV, and RH, similar to Adames and Wallace (2015). The three parameters are linked physically, as upward vertical motion transports water vapor from the boundary layer into the free troposphere (Fritz and Wang 2014), and rising motion and latent heat release lower surface pressure.

3.2.4 | Vertical Wind Shear

During the pre-monsoon period, VWS anomalies were statistically significant and largest when index amplitudes are greater than 2 (Figure 4e). They were negative (2–4 m s^{-1} below normal) on days when RMM2 is negative, and they were positive (3–5 m s^{-1} above normal) on days when RMM2 is positive. During the post-monsoon period, VWS anomalies were statistically significantly negative (1–3 m s^{-1} below normal) on days when the index amplitude is between 1 and 2 in Phases 7–3 (Figure 4f) and positive (3–5 m s^{-1} above normal) on days when the index amplitude is greater than 1 and in Phases 4–6, especially in Phase 5. Here, we show that VWS anomalies extend across much of the RMM phase space during both pre- and post-monsoon periods, building upon the work of Girishkumar et al. (2015), who found below-normal VWS supporting anomalous cyclogenesis during Phases 3–4.

3.2.5 | Sea Surface Temperature

During the pre-monsoon period, SST anomalies were statistically significantly positive (up to 1°C above normal) on days when RMM2 is negative and negative (up to −0.75°C below normal) on days when RMM2 is positive (Figure 4g). During the post-monsoon period, the SST anomaly picture is much less clear, with most of the phase space—especially when RMM2 is positive—not associated with statistically significant anomalies. SSTs were above normal on days when the index amplitude is greater than 1 and in Phases 1–2; SSTs were below normal on days when the index amplitude is greater than 1 and in Phases 7–8 (Figure 4h).

These results differ from Girishkumar and Ravichandran (2012) and Bhardwaj et al. (2019), who found higher SSTs in the BoB on pre-monsoon days when the index is in Phases 3–4 and concluded that intraseasonal variability in SSTs supports anomalous cyclogenesis. Here, pre-monsoon SST anomalies were positive on days when RMM2 is negative, but this includes a much broader region of phase space, not only Phases 3–4. Furthermore, the largest SST

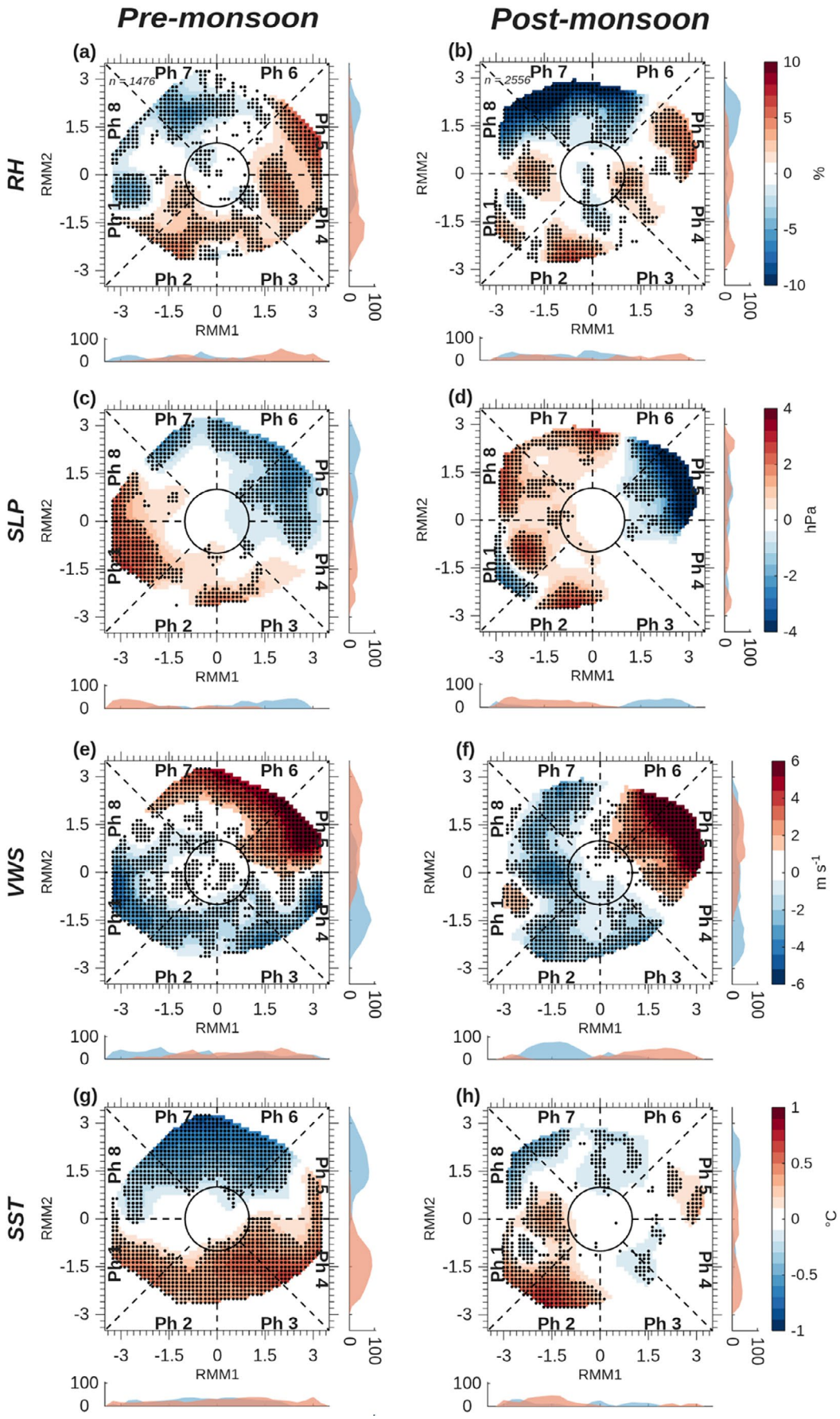

FIGURE 4 | As in Figure 3, but for anomalies of (a, b) relative humidity (RH) (averaged from 850–500 hPa, in %), (c, d) sea level pressure (SLP) (in hPa), (e, f) vertical wind shear (VWS) (between 200 and 850 hPa, in m s^{-1}), and (g, h) sea surface temperature (SST) (in °C).

anomalies occurred on days when the index amplitude is greater than 2, a result not found in earlier studies.

3.3 | Skill Scores

The POD, a measure of the fraction of the statistically significant anomalies of tropical cyclogenesis co-located in RMM phase space with statistically significant anomalies of each environmental parameter, ranged from 1.1% to 60.7% (Figure 5). The 700-hPa VV had the highest POD in both the pre- (50.0%) and post-monsoon (60.7%) periods, indicating that the VV detected more of the intraseasonal signal for cyclogenesis than any other variable. The post-monsoon SST had the lowest POD (1.1%), indicating that in that period, the SST captured practically none of the intraseasonal signal for cyclogenesis. The POD for the other variables ranged from 10% to 30%, indicating some skill at detecting intraseasonal patterns of cyclogenesis.

The FAR, a measure of the fraction of each environmental anomaly not co-located with a statistically significant cyclogenesis anomaly, was generally high for all parameters and ranged from 82.3% to 99.7% (Figure 5). This means that most of the significant above- or below-normal environmental anomalies were not associated with anomalous cyclogenesis. The 700-hPa VV had the lowest post-monsoon FAR, indicating that it was more likely than the other parameters to be associated with anomalous cyclogenesis. The post-monsoon SST had a FAR near 100%, indicating that essentially none of the SST anomalies were associated with anomalous cyclogenesis.

The CSI, a measure of the accuracy of each environmental parameter in capturing the variability of cyclogenesis, was generally low and ranged from 0.003 to 0.148 (Figure 5). In the pre-monsoon period, the VV was the top-performing variable, with RH, SLP, and VWS only 50%–60% as accurate and SST only 44% as accurate. In the post-monsoon period, as in the pre-monsoon period, the VV performed best at capturing cyclogenesis. The RH and SLP were only 35%–40% as accurate as the VV, and the VWS and SST were worse, only 2%–16% as accurate.

Environmental parameters	Pre-monsoon			Post-monsoon		
	POD	FAR	CSI	POD	FAR	CSI
VV (700 hPa)	50.0	82.6	0.148	60.7	86.8	0.121
VV (500 hPa)	39.3	86.6	0.111	5.8	94.2	0.051
RH	27.4	88.4	0.089	17.5	93.7	0.049
SLP	21.9	87.8	0.085	19.3	94.5	0.045
VWS	29.3	90.9	0.074	10.5	97.6	0.020
SST	24.3	91.7	0.066	1.1	99.6	0.003

FIGURE 5 | Heat map of skill scores—the probability of detection (POD), false alarm rate (FAR), and critical success index (CSI)—between pre- and post-monsoon cyclogenesis anomalies and large-scale environmental parameters: The VV at 700 and 500 hPa, relative humidity (RH), sea level pressure (SLP), vertical wind shear (VWS), and sea surface temperature (SST).

4 | Summary and Conclusions

Anomalous probabilities of tropical cyclogenesis in the BoB were calculated across the phase space of the real-time multivariate MJO index for pre- and post-monsoon periods. Cyclogenesis anomalies were then compared to anomalies of four atmospheric and one oceanic parameter known to be related to TC formation. Skill scores were calculated to quantify the ability of each parameter to detect intraseasonal cyclogenesis. Anomalous probabilities of cyclogenesis were found to extend across the full RMM phase space, and cyclogenesis was favored in both pre- and post-monsoon periods when RMM1 is positive. On days when the intraseasonal index is in phases previously found favorable for cyclogenesis, anomalies are statistically significant for only a limited range of amplitudes. Moreover, MJO events with amplitudes > 2.0 seem to modulate cyclogenesis only in the pre-monsoon period, with little significant impact in the post-monsoon period.

The VV, RH, and SLP anomalies are most intense when the RMM index amplitude is largest. This is likely because the two principal components of the index are defined by spatial loading patterns of large-scale circulations that strongly project onto vertical motion, humidity, and surface pressure in the BoB (Roundy 2015). When these conditions overlap in phase space, cyclogenesis is favored. We thus recommend that intraseasonal predictions of cyclogenesis in the BoB consider not only the phase of the index but also the magnitude and sign of both RMM1 and RMM2.

The 700-hPa VV was found to have the highest POD, lowest FAR, and highest CSI of any other parameter, both in the pre- and post-monsoon periods, although all parameters had relatively high FAR and low CSI. When very strong RMM amplitudes (> 2.5) were excluded from analysis, the POD and CSI increased and FAR decreased (not shown), indicating that all parameters were relatively better at identifying cyclogenesis in the BoB during weaker MJO events. In the pre-monsoon period, the SLP, RH, VWS, and SST all had about half of the POD, higher FARs, and lower CSIs than the VV. The separation between VV and the other parameters is even more pronounced in the post-monsoon period. These results indicate that the VV is more skillful at detecting intraseasonal cyclogenesis in the BoB than RH, SLP, VWS, or SST, building on the work by Moon et al. (2018), Zhou and Li et al. (2019), and Wang and Murakami (2020), who identified 500-hPa VV as a predictor of intraseasonal cyclogenesis. However, here we found that in both pre- and post-monsoon periods, the 700-hPa VV outperformed the 500-hPa VV. This could be because 700-hPa VV is a more direct proxy for heat and moisture transport from the boundary layer into the free troposphere (e.g., Bretherton et al. 2004) and thus a better indicator of an environment favorable for deep convection and cyclogenesis (Wu et al. 2009; Wang 2014; Bui et al. 2016). The low skill of the post-monsoon VWS (0.02 CSI, less than 17% of VV) contrasts with Yanase et al. (2012), who found VWS to be a leading intraseasonal driver of cyclogenesis in October–November.

The poor performance of SST in detecting intraseasonal signals for cyclogenesis contrasts with Maneesha et al. (2025) and Suneeta et al. (2026) but agrees with Kushwaha et al. (2025), who found less contribution from the ocean and more from RH. SST may be a better discriminant when paired with other modes of variability, including the El Niño–Southern Oscillation and the Indian Ocean Dipole (Girishkumar

et al. 2015; Roose et al. 2022), the Pacific Decadal Oscillation (Roose et al. 2023), the quasi-biweekly oscillation (Chen et al. 2024), the Boreal Summer Intraseasonal Oscillation (BSISO; Kikuchi and Wang 2010), or other equatorial waves (Landu et al. 2020). Investigating those possible links is suggested for future work.

The results of this study are based on the RMM index, chosen because of its widespread adoption in both research and operations. Other MJO indices could be considered, including those based on outgoing longwave radiation (Kiladis et al. 2014) or the velocity potential (Ventrice et al. 2013). Follow-up studies could also examine variability across the phase space of the BSISO, as there is recent work suggesting that the BSISO is a better predictor of BoB cyclogenesis than the MJO in extended summer months (Kikuchi et al. 2012; Kikuchi 2021).

Author Contributions

Md Foysal: writing – review and editing. **Sahadat Habib:** writing – review and editing. **Md Hanif Biswas:** writing – review and editing. **Pallav Ray:** writing – review and editing. **Nadim Mahmud:** conceptualization, formal analysis, writing – review and editing, investigation, writing – original draft. **Bradford S. Barrett:** conceptualization, formal analysis, writing – original draft, writing – review and editing, investigation, methodology, project administration. **Md Masud-Ul-Alam:** conceptualization, methodology, writing – review and editing. **Most Israt Jahan Mili:** writing – review and editing.

Acknowledgments

IBTrACS was produced by a team of scientists from NOAA in collaboration with scientists worldwide. The RMM index was created by the Bureau of Meteorology of the Commonwealth of Australia. The results contain modified Copernicus Climate Change Service information. Neither the European Commission nor ECMWF is responsible for any use that may be made of the Copernicus information or data it contains.

Funding

The authors have nothing to report.

Conflicts of Interest

The authors declare no conflicts of interest.

Data Availability Statement

The data that support the findings of this study are available from the International Best Track Archive for Climate Stewardship, https://doi.org/10.25921/82ty-9e16, the real-time multivariate MJO index, https://doi.org/10.1175/1520-0493(2004)132%3C1917:AARMMI%3E2.0.CO;2, the fifth-generation global reanalysis produced by the European Centre for Medium-Range Weather Forecasts, https://doi.org/10.1002/qj.3803, and the global sea surface temperature analysis of the Copernicus Climate Change Service, https://doi.org/10.24381/cds.cf608234.

References

Adames, Á. F., and J. M. Wallace. 2015. "Three-Dimensional Structure and Evolution of the Moisture Field in the MJO." *Journal of the Atmospheric Sciences* 72, no. 10: 3733–3754. https://doi.org/10.1175/JAS-D-15-0003.1.

Alam, E., and D. Dominey-Howes. 2015. "A New Catalogue of Tropical Cyclones of the Northern Bay of Bengal and the Distribution and Effects of Selected Landfalling Events in Bangladesh." *International Journal of Climatology* 35, no. 6: 801–835. https://doi.org/10.1002/joc.4035.

Balaguru, K., S. Taraphdar, L. R. Leung, and G. R. Foltz. 2014. "Increase in the Intensity of Postmonsoon Bay of Bengal Tropical Cyclones." *Geophysical Research Letters* 41, no. 10: 3594–3601. https://doi.org/10.1002/2014GL060197.

Bao, J., S. Bony, D. Takasuka, and C. Muller. 2025. "Tropics-Wide Intraseasonal Oscillations." *Proceedings of the National Academy of Sciences of the United States of America* 122, no. 48: e2511549122. https://doi.org/10.1073/pnas.2511549122.

Bhardwaj, P., D. R. Pattanaik, and O. Singh. 2019. "Tropical Cyclone Activity Over Bay of Bengal in Relation to El Niño-Southern Oscillation." *International Journal of Climatology* 39, no. 14: 5452–5469. https://doi.org/10.1002/JOC.6165.

Bhardwaj, P., and O. Singh. 2020. "Climatological Characteristics of Bay of Bengal Tropical Cyclones: 1972–2017." *Theoretical and Applied Climatology* 139, no. 1: 615–629. https://doi.org/10.1007/s00704-019-02989-4.

Bretherton, C. S., M. E. Peters, and L. E. Back. 2004. "Relationships Between Water Vapor Path and Precipitation Over the Tropical Oceans." *Journal of Climate* 17, no. 7: 1517–1528. https://doi.org/10.1175/1520-0442(2004)017%3C1517:RBWVPA%3E2.0.CO;2.

Bui, H. X., J. Y. Yu, and C. Chou. 2016. "Impacts of Vertical Structure of Large-Scale Vertical Motion in Tropical Climate: Moist Static Energy Framework." *Journal of the Atmospheric Sciences* 73, no. 11: 4427–4437. https://doi.org/10.1175/JAS-D-16-0031.1.

Cao, Y. 2025. "Bivariant Kernel Density Estimation *MATLAB Central File Exchange*."

Chen, W., C. H. Ho, S. Yang, Z. Wu, and H. Chen. 2024. "Modulations of Madden–Julian Oscillation and Quasi-Biweekly Oscillation on Early Summer Tropical Cyclone Genesis Over the Bay of Bengal and South China Sea." *Journal of Climate* 37, no. 6: 1951–1964. https://doi.org/10.1175/JCLI-D-23-0376.1.

Duan, W., J. Yuan, X. Duan, and D. Feng. 2021. "Seasonal Variation of Tropical Cyclone Genesis and the Related Large-Scale Environments: Comparison Between the Bay of Bengal and Arabian Sea Sub-Basins." *Atmosphere* 12, no. 12: 1593. https://doi.org/10.3390/atmos12121593.

Embury, O., C. J. Merchant, S. A. Good, et al. 2024. "Satellite-Based Time-Series of Sea-Surface Temperature Since 1980 for Climate Applications." *Scientific Data* 11: 326. https://doi.org/10.1038/s41597-024-03147-w.

Fritz, C., and Z. Wang. 2014. "Water Vapor Budget in a Developing Tropical Cyclone and Its Implication for Tropical Cyclone Formation." *Journal of the Atmospheric Sciences* 71, no. 11: 4321–4332. https://doi.org/10.1175/JAS-D-13-0378.1.

Gahtan, J., K. R. Knapp, C. J. Schreck, et al. 2024. "International Best Track Archive for Climate Stewardship (IBTrACS) Project, Version 4.01." NOAA National Centers for Environmental Information, 10.25921/82ty-9e16.

Girishkumar, M. S., and M. Ravichandran. 2012. "The Influences of ENSO on Tropical Cyclone Activity in the Bay of Bengal during October–December." *Journal of Geophysical Research: Oceans* 117, no. C2. https://doi.org/10.1029/2011JC00741.

Girishkumar, M. S., K. Suprit, S. Vishnu, V. T. Prakash, and M. Ravichandran. 2015. "The Role of ENSO and MJO on Rapid Intensification of Tropical Cyclones in the Bay of Bengal During October–December." *Theoretical and Applied Climatology* 120, no. 3: 797–810. https://doi.org/10.1007/s00704-014-1214-z.

Gorja, M. M. K., N. K. Vissa, and Y. Viswanadhapalli. 2025. "Multi-Scale Atmospheric Interactions and Their Role in Modulating Pre-Monsoon Tropical Cyclone Movement: A Regional Modeling Approach." *Climate Dynamics* 63, no. 9: 366. https://doi.org/10.1007/s00382-025-07800-x.

Gottschalck, J., M. Wheeler, K. Weickmann, et al. 2010. "A Framework for Assessing Operational Madden–Julian Oscillation Forecasts: A CLIVAR MJO Working Group Project." *Bulletin of the American Meteorological Society* 91, no. 9: 1247–1258. https://doi.org/10.1175/2010BAMS2816.1.

Hersbach, H., B. Bell, P. Berrisford, et al. 2020. "The ERA5 Global Reanalysis." *Quarterly Journal of the Royal Meteorological Society* 146, no. 730: 1999–2049. https://doi.org/10.1002/qj.3803.

Hoarau, K., J. Bernard, and L. Chalonge. 2012. "Intense Tropical Cyclone Activities in the Northern Indian Ocean." *International Journal of Climatology* 32, no. 13: 1935–1945. https://doi.org/10.1002/joc.2406.

Hossain, M. S., M. S. Hossain, M. F. A. Akhi, M. A. Samad, and M. A. K. Mallik. 2024. "Understanding the Formation and Intensification Process of Several Cyclonic Systems Over the Bay of Bengal Using the Revised Genesis Potential Parameter Index." *Evergreen* 11: 736–755. https://doi.org/10.5109/7183355.

Ipsita, P., V. Rakesh, and G. N. Mohapatra. 2023. "Role of Ocean–Atmosphere Interactions on Contrasting Characteristics of Two Cyclones Over the Arabian Sea." *Meteorology and Atmospheric Physics* 135, no. 5: 50. https://doi.org/10.1007/s00703-023-00987-w.

Jiang, X., Á. F. Adames, D. Kim, et al. 2020. "Fifty Years of Research on the Madden-Julian Oscillation: Recent Progress, Challenges, and Perspectives." *Journal of Geophysical Research: Atmospheres* 125, no. 17: e2019JD030911. https://doi.org/10.1029/2019JD030911.

Kabir, R., E. A. Ritchie, and C. Stark. 2022. "Tropical Cyclone Exposure in the North Indian Ocean." *Atmosphere* 13, no. 9: 1421. https://doi.org/10.3390/atmos13091421.

Kelkar, R. R. 2019. "Satellite Meteorology in India: Its Beginning, Growth and Future." *Mausam* 70, no. 1: 1–14. https://doi.org/10.54302/mausam.v70i1.160.

Kikuchi, K. 2021. "The Boreal Summer Intraseasonal Oscillation (BSISO): A Review." *Journal of the Meteorological Society of Japan. Ser. II* 99, no. 4: 933–972. https://doi.org/10.2151/jmsj.2021-045.

Kikuchi, K., and B. Wang. 2010. "Formation of Tropical Cyclones in the Northern Indian Ocean Associated With Two Types of Tropical Intraseasonal Oscillation Modes." *Journal of the Meteorological Society of Japan. Ser. II* 88, no. 3: 475–496. https://doi.org/10.2151/JMSJ.2010-313.

Kikuchi, K., B. Wang, and Y. Kajikawa. 2012. "Bimodal Representation of the Tropical Intraseasonal Oscillation." *Climate Dynamics* 38, no. 9: 1989–2000. https://doi.org/10.1007/s00382-011-1159-1.

Kiladis, G. N., J. Dias, K. H. Straub, et al. 2014. "A Comparison of OLR and Circulation-Based Indices for Tracking the MJO." *Monthly Weather Review* 142, no. 5: 1697–1715. https://doi.org/10.1175/MWR-D-13-00301.1.

Kim, H., F. Vitart, and D. E. Waliser. 2018. "Prediction of the Madden–Julian Oscillation: A Review." *Journal of Climate* 31, no. 23: 9425–9443. https://doi.org/10.1175/JCLI-D-18-0210.1.

Kim, M., D. Kang, S. J. Sohn, G. Kim, J. Rhee, and S. Kim. 2026. "Multi-Scale Decomposition for Skillful All-Season MJO Prediction With Deep Learning." *Geophysical Research Letters* 53, no. 1: e2025GL117981. https://doi.org/10.1029/2025GL117981.

Knapp, K. R., M. C. Kruk, D. H. Levinson, H. J. Diamond, and C. J. Neumann. 2010. "The International Best Track Archive for Climate Stewardship (IBTrACS)." *Bulletin of the American Meteorological Society* 91, no. 3: 363–376. https://doi.org/10.1175/2009BAMS2755.1.

Krishnamohan, K. S., K. Mohanakumar, and P. V. Joseph. 2012. "The Influence of Madden–Julian Oscillation in the Genesis of North Indian Ocean Tropical Cyclones." *Theoretical and Applied Climatology* 109, no. 1: 271–282. https://doi.org/10.1007/s00704-011-0582-x.

Kushwaha, V. K., V. K. Singh, A. Parekh, and C. Gnanaseelan. 2025. "Revisiting the Tropical Cyclone Genesis Potential Index for the Bay of Bengal Post-Monsoon Season." *Journal of Earth System Science* 134, no. 3: 153. https://doi.org/10.1007/s12040-025-02617-y.

Lafleur, D. M., B. S. Barrett, and G. R. Henderson. 2015. "Some Climatological Aspects of the Madden–Julian Oscillation (MJO)." *Journal of Climate* 28, no. 15: 6039–6053. https://doi.org/10.1175/JCLI-D-14-00744.1.

Landu, K., R. Goyal, and B. S. Keshav. 2020. "Role of Multiple Equatorial Waves on Cyclogenesis Over Bay of Bengal." *Climate Dynamics* 54, no. 3: 2287–2296. https://doi.org/10.1007/s00382-019-05112-5.

Li, Z., W. Yu, K. Li, H. Wang, and Y. Liu. 2019. "Environmental Conditions Modulating Tropical Cyclone Formation Over the Bay of Bengal During the Pre-Monsoon Transition Period." *Journal of Climate* 32, no. 14: 4387–4394. https://doi.org/10.1175/JCLI-D-18-0620.1.

Madden, R. A., and P. R. Julian. 1971. "Detection of a 40–50 Day Oscillation in the Zonal Wind in the Tropical Pacific." *Journal of the Atmospheric Sciences* 28, no. 4: 702–708. https://doi.org/10.1175/1520-0469(1971)028%3C0702:DOADOI%3E2.0.CO;2.

Madden, R. A., and P. R. Julian. 1972. "Description of Global-Scale Circulation Cells in the Tropics With a 40–50 Day Period." *Journal of Atmospheric Sciences* 29, no. 6: 1109–1123. https://doi.org/10.1175/1520-0469(1972)029<1109:DOGSCC>2.0.CO;2.

Maneesha, K., K. V. K. R. K. Patnaik, P. Ganapathi, and S. B. Ratna. 2025. "Pre-Requisite Conditions for the Intensification of Pre-Monsoon Cyclones Over the Bay of Bengal." *Scientific Reports* 15, no. 1: 33049. https://doi.org/10.1038/s41598-025-05121-x.

Matin, N., M. E. H. Sakib, and G. M. J. Hasan. 2024. "Vulnerability Assessment of Tropical Cyclones and Deep Depressions: An Index-Based Spatio-Temporal Assessment Along the Coastal Zones of Bangladesh." *Natural Hazards* 120, no. 5: 4367–4388. https://doi.org/10.1007/s11069-023-06380-5.

Mittal, R., M. Tewari, C. Radhakrishnan, P. Ray, T. Singh, and A. K. Nickerson. 2019. "Response of Tropical Cyclone Phailin (2013) in the Bay of Bengal to Climate Perturbations." *Climate Dynamics* 53, no. 3: 2013–2030. https://doi.org/10.1007/s00382-019-04761-w.

Moon, J. Y., B. Wang, S. S. Lee, and K. J. Ha. 2018. "An Intraseasonal Genesis Potential Index for Tropical Cyclones During Northern Hemisphere Summer." *Journal of Climate* 31, no. 22: 9055–9071. https://doi.org/10.1175/JCLI-D-18-0515.1.

Pal, A., and S. Chatterjee. 2021. "Influence of Seasonal Variability in the Environmental Factors on Tropical Cyclone Activity Over the Bay of Bengal Region." *Spatial Information Research* 29, no. 5: 673–684. https://doi.org/10.1007/s41324-021-00383-9.

Paul, D., J. Panda, S. Mandke, A. Routray, and Y. J. Zhu. 2025. "Investigating Concurrent Cyclonic Disturbances in the North Indian Ocean and Associated Large-Scale Atmospheric Influences." *Journal of Applied Meteorology and Climatology* 64, no. 9: 1271–1290. https://doi.org/10.1175/JAMC-D-24-0148.1.

Rahul, R., J. Kuttippurath, A. Chakraborty, and R. S. Akhila. 2022. "The Inverse Influence of MJO on the Cyclogenesis in the North Indian Ocean." *Atmospheric Research* 265: 105880. https://doi.org/10.1016/j.atmosres.2021.105880.

Robertson, A. W., F. Vitart, and S. J. Camargo. 2020. "Subseasonal to Seasonal Prediction of Weather to Climate With Application to Tropical Cyclones." *Journal of Geophysical Research: Atmospheres* 125, no. 6: e2018JD029375. https://doi.org/10.1029/2018JD029375.

Roman-Stork, H. L., and B. Subrahmanyam. 2020. "The Impact of the Madden–Julian Oscillation on Cyclone Amphan (2020) and Southwest Monsoon Onset." *Remote Sensing* 12, no. 18: 3011. https://doi.org/10.3390/rs12183011.

Roose, S., R. S. Ajayamohan, P. Ray, et al. 2023. "Pacific Decadal Oscillation Causes Fewer Near-Equatorial Cyclones in the North Indian

Ocean." *Nature Communications* 14, no. 1: 5099. https://doi.org/10.1038/s41467-023-40642-x.

Roose, S., R. S. Ajayamohan, P. Ray, P. R. Mohan, and K. Mohanakumar. 2022. "ENSO Influence on Bay of Bengal Cyclogenesis Confined to Low Latitudes." *npj Climate and Atmospheric Science* 5, no. 1: 31. https://doi.org/10.1038/s41612-022-00252-8.

Roundy, P. E. 2015. "On the Interpretation of EOF Analysis of ENSO, Atmospheric Kelvin Waves, and the MJO." *Journal of Climate* 28, no. 3: 1148–1165. https://doi.org/10.1175/JCLI-D-14-00398.1.

Sattar, A. M., and K. K. Cheung. 2019. "Comparison Between the Active Tropical Cyclone Seasons Over the Arabian Sea and Bay of Bengal." *International Journal of Climatology* 39, no. 14: 5486–5502. https://doi.org/10.1002/joc.6167.

Schreck, C. J., III, F. Vitart, S. J. Camargo, et al. 2023. "Advances in Tropical Cyclone Prediction on Subseasonal Time Scales During 2019–2022." *Tropical Cyclone Research and Review* 12, no. 2: 136–150. https://doi.org/10.1016/j.tcrr.2023.06.004.

Singh, V. K., M. K. Roxy, and M. Deshpande. 2021. "Role of Warm Ocean Conditions and the MJO in the Genesis and Intensification of Extremely Severe Cyclone Fani." *Scientific Reports* 11, no. 1: 3607. https://doi.org/10.1038/s41598-021-82680-9.

Suneeta, P., T. U. Bhaskar, and S. S. V. S. Ramakrishna. 2026. "Impact of ENSO on the Genesis Potential Index of Cyclones Over the Bay of Bengal During the Post-Monsoon Season." *Dynamics of Atmospheres and Oceans* 113: 101642. https://doi.org/10.1016/j.dynatmoce.2025.101642.

Taylor, H. T., B. Ward, M. Willis, and W. Zaleski. 2010. *The Saffir-Simpson Hurricane Wind Scale*. National Oceanic and Atmospheric Administration.

Tromeur, E., and W. B. Rossow. 2010. "Interaction of Tropical Deep Convection With the Large-Scale Circulation in the MJO." *Journal of Climate* 23, no. 7: 1837–1853. https://doi.org/10.1175/2009JCLI3240.1.

Tsuboi, A., and T. Takemi. 2014. "The Interannual Relationship Between MJO Activity and Tropical Cyclone Genesis in the Indian Ocean." *Geoscience Letters* 1, no. 1: 9. https://doi.org/10.1186/2196-4092-1-9.

Ventrice, M. J., M. C. Wheeler, H. H. Hendon, C. J. Schreck III, C. D. Thorncroft, and G. N. Kiladis. 2013. "A Modified Multivariate Madden–Julian Oscillation Index Using Velocity Potential." *Monthly Weather Review* 141, no. 12: 4197–4210. https://doi.org/10.1175/MWR-D-12-00327.1.

Wahiduzzaman, M., and A. Yeasmin. 2024. "An Assessment of Tropical Cyclone Frequency in the Bay of Bengal and Its Impact on Coastal Bangladesh." *Coasts* 4, no. 3: 594–608. https://doi.org/10.3390/coasts4030030.

Wang, B., and H. Murakami. 2020. "Dynamic Genesis Potential Index for Diagnosing Present-Day and Future Global Tropical Cyclone Genesis." *Environmental Research Letters* 15, no. 11: 114008. https://doi.org/10.1088/1748-9326/abbb01.

Wang, Z. 2014. "Role of Cumulus Congestus in Tropical Cyclone Formation in a High-Resolution Numerical Model Simulation." *Journal of the Atmospheric Sciences* 71, no. 5: 1681–1700. https://doi.org/10.1175/JAS-D-13-0257.1.

Wheeler, M. C., and H. H. Hendon. 2004. "An All-Season Real-Time Multivariate MJO Index: Development of an Index for Monitoring and Prediction." *Monthly Weather Review* 132, no. 8: 1917–1932. https://doi.org/10.1175/1520-0493(2004)132<1917:AARMMI>2.0.CO;2.

Wilks, D. S. 2011. *Statistical Methods in the Atmospheric Sciences*. 2nd ed, 627. Academic Press.

Wu, C. M., B. Stevens, and A. Arakawa. 2009. "What Controls the Transition From Shallow to Deep Convection?" *Journal of the Atmospheric Sciences* 66, no. 6: 1793–1806. https://doi.org/10.1175/2008JAS2945.1.

Yanase, W., M. Satoh, H. Taniguchi, and H. Fujinami. 2012. "Seasonal and Intraseasonal Modulation of Tropical Cyclogenesis Environment Over the Bay of Bengal During the Extended Summer Monsoon." *Journal of Climate* 25, no. 8: 2914–2930. https://doi.org/10.1175/JCLI-D-11-00208.1.

Zhao, C., and T. Li. 2019. "Basin Dependence of the MJO Modulating Tropical Cyclone Genesis." *Climate Dynamics* 52, no. 9: 6081–6096. https://doi.org/10.1007/s00382-018-4502-y.

Zhou, Z., W. Duan, R. Yang, X. Qin, and Y. Li. 2025. "Uncertainty of "Pangu-Weather" in Bay of Bengal Storm Track Forecasts: Target Observation Perspective." *Atmospheric Research* 326: 108313. https://doi.org/10.1016/j.atmosres.2025.108313.